# Expression, Purification, and Inhibitory Properties of Human Proteinase Inhibitor 8†

Jeffrey R. Dahlen,‡ Donald C. Foster,§ and Walter Kisiel*,‡

*Department of Pathology, University of New Mexico School of Medicine, Albuquerque, New Mexico 87131, and ZymoGenetics, Inc., Seattle, Washington 98102*

*Received April 25, 1997; Revised Manuscript Received September 22, 1997*⊗

ABSTRACT: In a previous report, the cDNA for human proteinase inhibitor 8 (PI8) was first identified, isolated, and subcloned into a mammalian expression vector and expressed in baby hamster kidney cells. Initial studies indicated that PI8 was able to inhibit the amidolytic activity of trypsin and form an SDS-stable ~67-kDa complex with human thrombin [Sprecher, C. A., et al. (1995) *J. Biol Chem. 270*, 29854−29861]. In the present study, we have expressed recombinant PI8 in the methylotropic yeast *Pichia pastoris*, purified the inhibitor to homogeneity, and investigated its ability to inhibit a variety of proteinases. PI8 inhibited the amidolytic activities of porcine trypsin, human thrombin, human coagulation factor Xa, and the *Bacillus subtilis* dibasic endoproteinase subtilisin A through different mechanisms but failed to inhibit the *Staphylococcus aureus* endoproteinase Glu-C. PI8 inhibited trypsin in a purely competitive manner, with an equilibrium inhibition constant ($K_i$) of less than 3.8 nM. The interaction between PI8 and thrombin occurred with a second-order association rate constant ($k_{assoc}$) of $1.0 \times 10^5$ $M^{-1}$ $s^{-1}$ and a $K_i$ of 350 pM. A slow-binding kinetics approach was used to determine the kinetic constants for the interactions of PI8 with factor Xa and subtilisin A. PI8 inhibited factor Xa via a two-step mechanism with a $k_{assoc}$ of $7.5 \times 10^4$ $M^{-1}$ $s^{-1}$ and an overall $K_i$ of 272 pM. PI8 was a potent inhibitor of subtilisin A via a single-step mechanism with a $k_{assoc}$ of $1.16 \times 10^6$ $M^{-1}$ $s^{-1}$ and an overall $K_i$ of 8.4 pM. The interaction between PI8 and subtilisin A may be of physiological significance, since subtilisin A is an evolutionary precursor to the intracellular mammalian dibasic processing endoproteinases.

The mammalian serine proteinase inhibitors, or serpins, are a superfamily of proteins that range from 40 to 60 kDa in molecular mass, resemble $\alpha_1$-proteinase inhibitor in overall structure, and include a number of homologous proteins such as $\alpha_1$-antichymotrypsin, $\alpha_2$-antiplasmin, antithrombin III, and plasminogen activator inhibitors 1 and 2 (*1*). Serpins regulate a wide variety of physiological processes that involve proteinase activity including, but not limited to, blood coagulation, complement activation, cell migration and differentiation, intracellular proteolysis, and fibrinolysis (*2*). Serpins inhibit their target proteinases by forming a 1:1 stoichiometric complex with the active site of the proteinase, which is, in most cases, resistant to denaturants (*3*). Serpins are composed of three $\beta$-sheets surrounded by eight α-helices, and their proteinase-inhibitory specificity is determined by the $P_1-P_1'$ residues located within the reactive site loop (*1*, *4*, *5*). The reactive site loop is highly divergent among serpin family members and exists as a stressed loop with a canonical conformation that confers the optimal conformation for high-affinity association with the substrate binding cleft of the cognate proteinase, with the $P_1-P_1'$ residues acting as a pseudosubstrate for the target proteinase (*6*). Unlike a typical substrate, the serpin has the ability to form a tight complex that may be essential for inactivation of the proteinase (*4*, *7*−*9*). Most serpins can interact with more than one proteinase *in vitro*, but the affinity of such interactions must be determined in order to suggest physiological relevance.

Separate from the serpins that regulate proteinase activity are several members that lack proteinase inhibitory ability and have other physiological roles. These serpins were originally identified through database searches and include thyroxine-binding globulin (*10*), angiotensinogen (*11*), and ovalbumin (*12*). Ovalbumin represents the parent prototype of a unique family of serpins that lack a typical cleavable amino-terminal signal sequence but have been found to reside intracellularly (*13*, *14*), extracellularly, or both (*15*−*18*). Therefore, it can be inferred that the functions of members of the ovalbumin family of serpins may not be strictly confined to the cytoplasm. The serpins previously classified as members of the ovalbumin family of serpins are plasminogen activator inhibitor-2 (PAI-2)[1] (*18*), an elastase inhibitor (EI) isolated from monocyte-like cells (*19*, *20*), squamous cell carcinoma antigen (SCCA) (*16*), maspin (*21*), proteinase inhibitor 6 (PI6) (*22*−*24*), two serpins first identified by this laboratory, proteinase inhibitor 8 (PI8) (*25*) and proteinase inhibitor 9 (PI9) (*14*, *25*), squamous cell carcinoma antigen 2 (SCCA2) (*26*), and bomapin (*27*). PI6, PI8, and PI9 are

† Supported in part by grant HL35246 from the National Institutes of Health.

* Corresponding author: Walter Kisiel, Ph.D. Department of Pathology, University of New Mexico School of Medicine, Albuquerque, NM 87131. Tel.: (505) 272-0094. Fax: (505) 272-5139. E-mail: wkisiel@medusa.unm.edu.

‡ University of New Mexico School of Medicine.

§ ZymoGenetics, Inc.

⊗ Abstract published in *Advance ACS Abstracts,* November 15, 1997.

[1] Abbreviations used: PI8, proteinase inhibitor 8; PAI-2, plasminogen activator inhibitor 2; EI, elastase inhibitor; SCCA, squamous cell carcinoma antigen; PI6, proteinase inhibitor 6; PI9, proteinase inhibitor 9; SDS, sodium dodecyl sulfate; *p*-NPGB, *p*-nitrophenyl *p*-guanidinobenzoate; Z-FLE-*p*NA, carbobenzoxy-Phe-Leu-Glu-*p*-nitroanilide; Suc-AAPF-*p*NA, succinyl-Ala-Ala-Pro-Phe-*p*-nitroanilide; S-2288, H-D-Ile-Pro-Arg-*p*-nitroanilide; S-2765, N-α-Cbo-D-Arg-Gly-Arg-*p*-nitroanilide; FPLC, fast protein liquid chromatography; DTT, dithiothreitol; PMSF, phenylmethylsulfonyl fluoride; BSA, bovine serum albumin; DMSO, dimethlyl sulfoxide; DMF, dimethyl formamide.

S0006-2960(97)00977-X CCC: $14.00 

unique among the mammalian ovalbumin-type serpins in that they contain a cysteine residue in the $P_1'$ position within the reactive site loop, which is also present in the viral serpin CrmA (*25*). It has been demonstrated that individual mammalian ovalbumin-type serpins can inhibit a variety of prototypic serine proteinases (*22*, *23*, *26*), and in some cases, they have been shown to exhibit cross-class specificity and inhibit intracellular cysteine proteinases (*28*). Thus, serpins may function not only by distinctly different mechanisms using a variety of kinetic parameters to regulate physiological proteolysis (*29*) but also by interacting with distinctly different types of proteinases. Although most members of the ovalbumin family of serpins exhibit defined proteinase inhibitory activity, the true physiological targets of these serpins have not yet been identified. PI8 is a serpin composed of 374 amino acids with a molecular mass of ~45 kDa whose transcript can be found in a variety of tissues and was first identified by screening a human placental $\lambda$gt11 cDNA library using a probe corresponding to an internal sequence of PI6. PI8 has also been demonstrated to have inhibitory activity toward trypsin and the ability to form an SDS-stable 67-kDa complex with human thrombin (*25*). In this study, we have expressed functionally active PI8 in the methylotropic yeast *Pichia pastoris* and purified the inhibitor to homogeneity. In addition, we have performed a detailed kinetic analysis of the inhibitory properties of PI8 using porcine trypsin, human thrombin, human coagulation factor Xa, and the evolutionarily divergent subtilisin A from *B. subtilis* as model serine proteinases.

## MATERIALS AND METHODS

*Materials.* The *Pichia* expression kit, including the expression vector pPIC3, *P. pastoris* strain GS115, and all yeast growth media components were purchased from Invitrogen (San Diego, CA). The restriction endonucleases *Avr*II, *Bam*HI, *Bgl*II, *Eco*RI, *Not*I, and *Xba*I were purchased from New England Biolabs (Beverly, MA). Qiagen-tip columns were purchased from Qiagen, Inc. (Chatsworth, CA). A Bead Beater apparatus and zirconia/silica beads were purchased from BioSpec, Inc. (Bartlesville, OK). Hepes buffer, dithiothreitol (DTT), leupeptin, pepstatin, phenylmethylsulfonyl fluoride (PMSF), bovine serum albumin (BSA), benzamidine, heparin, dimethlyl sulfoxide (DMSO), dimethyl formamide (DMF) and *p*-nitrophenyl *p*-guanidinobenzoate (*p*-NPGB) were purchased from Sigma Chemical Co. (St. Louis, MO). Porcine trypsin was obtained from Novo Nordisk (Bagsvaerd, Denmark). $\alpha_2$-Macroglobulin and carbobenzoxy-Phe-Leu-Glu-*p*-nitroanilide (Z-FLE-*p*NA) were purchased from Boehringer Mannheim (Indianapolis, IN). *S. aureus* endoproteinase Glu-C was purchased from Worthington Biochemical Corp. (Freehold, NJ). Subtilisin A was generously provided by Lene Adamczewski from Novo Nordisk A/S (Bagsvaerd, Denmark). Succinyl-Ala-Ala-Pro-Phe-*p*-nitroanilide (Suc-AAPF-*p*NA) was obtained from Calbiochem-Novabiochem International (San Diego, CA). H-D-Ile-Pro-Arg-*p*-nitroanilide (S-2288) and N-$\alpha$-Cbo-D-Arg-Gly-Arg-*p*-nitroanilide (S-2765) were products of Kabi Pharmacia Hepar, Inc. (Franklin, OH). Heparin-agarose was prepared essentially as described (*30*). Human thrombin (*31*), human factor Xa (*32*), and antithrombin III (*33*) were prepared according to published procedures. UltraFit 3.0 software was purchased from Biosoft (Ferguson, MO).

*cDNA Cloning.* The 1.2 kilobase cDNA for PI8 was liberated from the Zem219b vector (previously described as Zem229R (*25*)) by restriction endonuclease digestion with *Bam*HI and *Xba*I. The PI8 cDNA was isolated and directionally cloned into the *P. pastoris* expression vector pPIC3 that had been previously digested with *Bam*HI and *Avr*II. The presence of the PI8 cDNA in the correct orientation in pPIC3 was verified by restriction endonuclease digestion with *Eco*RI and *Not*I. The resulting PI8/pPIC3 plasmid was digested with *Bgl*II and purified using a Qiagen-tip column according to the manufacturer's instructions.

*Transformation of Yeast and Analysis of Transformants.* Spheroplasts of the histidine-requiring *P. pastoris* strain GS115 (*his4*) were prepared and transformed with purified *Bgl*II-digested PI8/pPIC3 DNA according to the manufacturer's instructions. $His^+$ transformants were selected by plating on regeneration medium lacking histidine. All liquid cultures were grown on a shaking incubator (250−300 rpm) at 30 °C. Plates were also grown at 30 °C. The Mut phenotype of the $His^+$ transformants was determined by comparing growth rates of colonies streaked on media containing dextrose as the sole carbon source (MD) to media containing methanol as the sole carbon source (MM). Slower growth of transformants on MM media as compared to growth on MD media indicates a loss of the alcohol oxidase locus *AOX1* and gene replacement with the PI8 cDNA under control of the *AOX1* promoter ($P_{AOX1}$), resulting in a methanol utilization slow ($Mut^s$) phenotype. Identical growth rates were characterized as $Mut^+$.

*Expression and Purification of Recombinant Human PI8.* Single colonies of various $His^+$ transformants with different Mut phenotypes were grown to an $OD_{600} \approx 3$ in minimal medium containing glycerol (MGY). The cultures were centrifuged and resuspended to an $OD_{600} \approx 1$ in minimal medium containing 2.5% yeast nitrogen base and 0.5% methanol as the sole carbon source to induce expression of PI8. Cultures were grown for 2 days ($Mut^+$) or 5 days ($Mut^s$) with methanol added to 0.5% every 24 h to maintain induction. The cells were harvested by centrifugation (2000*g*; 5 min; 25 °C) in a Beckman J-6M/E centrifuge and resuspended in breaking buffer (50 mM Hepes (pH 7)/1 mM DTT/1 mM EDTA/1 mM PMSF/2 $\mu$g/mL of leupeptin/2 $\mu$g/mL of pepstatin) at 1/25 of the original culture volume. Cells were disrupted by vortexing with an equal volume of zirconia/silica beads for 30 s followed by 30 s incubation on ice for a total of eight cycles. The lysates were microcentrifuged, and the level of PI8 expression in the various transformants was determined by SDS-PAGE using 11% polyacrylamide slab gels (*34*). Gels were stained with 0.2% Coomassie Blue G-250 in 50% methanol/10% glacial acetic acid. A single $His^+$ $Mut^s$ clone with a high level of PI8 expression was selected for the eventual purification of PI8. A single colony of this clone was used to inoculate 20 mL of MGY and was cultured to an $OD_{600} \approx 5$. This 20 mL culture was then used to inoculate 2 L of MGY and was cultured to an $OD_{600} \approx 3$. Cells were harvested by centrifugation and resuspended in 1.5 L of MM containing 0.6% methanol. Cultures were grown for 5 days at 30 °C with methanol added to 0.5% every 24 h. After 5 days, cells were harvested by centrifugation and stored at −80 °C.

The yeast cell pellet was thawed, and cells were resuspended to an $OD_{600} \approx 75$ in breaking buffer (50 mM Hepes (pH 7)/1 mM DTT/2 mM EDTA/50 mM benzamidine/2 mM

PMSF/2 $\mu$g/mL of leupeptin/2 $\mu$g/mL of pepstatin). Cells were disrupted with an equal volume of zirconia/silica beads for 10 min in a Bead Beater apparatus. The lysate was centrifuged twice (10000*g*; 20 min; 4 °C) in a Beckman J2-21 centrifuge, and the supernatant was applied to a 2.6 × 35 cm heparin-agarose column previously equilibrated at 4 °C with 50 mM Hepes (pH 7) containing 1 mM DTT and 3 mM benzamidine at a flow rate of 1 mL/min. The column was washed with equilibrating buffer containing 1 mM PMSF, and PI8 was subsequently eluted at approximately 0.3 M NaCl in a linear NaCl gradient (0−0.6 M) dissolved in equilibrating buffer containing 1 mM PMSF. Fractions were tested for inhibitory activity toward trypsin at a dilution such that the inhibitory activity of PMSF was eliminated, and those fractions demonstrating inhibitory activity were pooled and dialyzed at 4 °C against 25 mM Tris-HCl (pH 8) containing 1 mM DTT. The dialyzed sample was concentrated by ultrafiltration, and 20% of the sample was applied to a Mono Q HR5/5 column (Pharmacia Biotech; Piscataway, NJ) previously equilibrated at room temperature with 25 mM Tris-HCl (pH 8)/1 mM DTT at a flow rate of 0.5 mL/min. PI8 was eluted from the column at approximately 0.25 M NaCl in a linear NaCl gradient (0−1 M) dissolved in equilibrating buffer. PI8-containing fractions were diluted 3-fold in 25 mM Tris-HCl (pH 7) containing 1 mM DTT and applied to a Mono S HR5/5 column (Pharmacia Biotech; Piscataway, NJ) previously equilibrated at room temperature with 25 mM Tris-HCl (pH 7) containing 1 mM DTT at a flow rate of 1 mL/min. PI8 was eluted at approximately 0.2 M NaCl, pH ~7.2 in a linear gradient (0−1 M NaCl, pH 7−pH 8) in 25 mM Tris-HCl/1 mM DTT. Fractions were analyzed by SDS-PAGE, and pure fractions were stored in aliquots at −80 °C.

*General Kinetic Methods.* The concentrations of catalytically active porcine trypsin and human thrombin were determined by titration with *p*-NPGB as previously described (*35*, *36*). Active site-titrated trypsin was used to titrate $\alpha_2$-macroglobulin, which was then used to determine the catalytically active concentration of subtilisin A. Active site-titrated human thrombin was used to titrate antithrombin III in the presence of 6.7 units/mL of heparin, which was then used to determine the catalytically active concentration of factor Xa, also in the presence of 6.7 units/mL of heparin as described (*22*). The active site-titrated enzymes were used to determine the amount of PI8 necessary for a 1:1 molar binding stoichiometry for the determination of kinetic constants. Trypsin (5 nM) was mixed with increasing amounts of PI8 in a total volume of 190 $\mu$L of 20 mM Hepes (pH 7.5)/0.15 M NaCl/0.01% BSA in individual wells of a microtitration plate previously blocked with buffer containing 0.1% BSA. The reactants were incubated for 15 min at 37 °C, and residual amidolytic activity was measured by adding 10 $\mu$L of 5 mM S-2288 dissolved in buffer for a final concentration of 0.25 mM and monitoring the enzymatic production of *p*-nitroaniline for 5 min at 405 nm using a $UV_{max}$ kinetic microtitration plate autoreader (Molecular Devices, Inc.; Menlo Park, CA). The data were fitted to the Hill equation for inhibitor-concentration dependence (*37*)

$$\nu = \frac{\nu_o}{1 + \left(\frac{[I]}{K_{0.5}}\right)^h} \quad (1)$$

where $\nu$ is the inhibited rate, $\nu_o$ is the uninhibited rate, [I] is the amount of PI8 present, $K_{0.5}$ is the amount of PI8 required to produce $\nu = \nu_o/2$, and $h$ is the slope of the line produced by a plot of $\log[\nu/(\nu_o - \nu)]$ against log [I]. $K_{0.5}$ was determined by regression analysis using UltraFit 3.0 software to measure the amount of PI8 required to produce $\nu = \nu_o/2$. The amount of PI8 used for an equimolar concentration with trypsin (5 nM) in further studies was equal to $2K_{0.5}$. The reactive concentration of PI8 was measured by titration with subtilisin A by incubating increasing amounts of PI8 with enzyme (5 nM) in a total volume of 180 $\mu$L of 20 mM Hepes (pH 7.5)/0.15 M NaCl/0.01% BSA in individual wells of a microtitration plate previously blocked with buffer containing 0.1% BSA. The reactants were incubated for 30 min at 37 °C, and residual amidolytic activity was measured by adding 20 $\mu$L of 2 mM Suc-AAPF-*p*NA in 0.1 M Hepes/0.5 M NaCl/20% DMSO for a final concentration of 0.2 mM and monitoring $\Delta A_{405}$/min using the microplate reader. The data were used to plot the enzymatic rate of substrate hydrolysis as a function of the amount of PI8 added to the reaction well. Linear regression to the *x*-axis was used to calculate the precise amount of PI8 required to form a 1:1 stoichiometric complex. This approach was also used to determine the amount of PI8 required to form a 1:1 stoichiometric complex with factor Xa and thrombin using S-2765 (0.2 mM final concentration) and S-2288 (0.25 mM) as substrates, respectively.

Enzyme−substrate catalytic constants were measured at 25 °C in 20 mM Hepes (pH 7.5)/0.15 M NaCl/0.01% BSA containing 2% DMSO and 1% DMF to ensure solubility of substrate during the reactions. Data were fitted to the Michaelis−Menton equation using UltraFit software to determine values for $K_m$ and $k_{cat}$. The catalytic constants for subtilisin A and Suc-AAPF-*p*NA were $K_m = 0.195$ mM and $k_{cat} = 379$ s$^{-1}$. The catalytic constants for trypsin and S-2288 were $K_m = 0.015$ mM and $k_{cat} = 140$ s$^{-1}$. The catalytic constants for thrombin and S-2288 were $K_m = 0.009$ mM and $k_{cat} = 101$ s$^{-1}$. The catalytic constants for factor Xa and S-2765 were $K_m = 0.145$ mM and $k_{cat} = 297$ s$^{-1}$.

*Determination of Inhibition Constants for PI8 with Trypsin and Thrombin.* Trypsin (24 $\mu$L; 5 nM final concentration) was added to 176 $\mu$L of buffer (20 mM Hepes (pH 7.5)/0.15 M NaCl/0.01% BSA) containing increasing concentrations of substrate mixed with 0, 5, and 7.5 nM PI8. Trypsin amidolytic activity was measured by the microplate reader from $\Delta A_{405}$/min. The data obtained were used to determine the upper limit of the inhibition constant ($K_i$) from a double-reciprocal plot of 1/rate against 1/[S-2288].

The overall equilibrium inhibition constant ($K_i$) and the second-order association rate constant ($k_{assoc}$) for the inhibition of thrombin by PI8 were determined as follows. Equimolar concentrations of thrombin and PI8 were incubated at 25 °C in 190 $\mu$L of 20 mM Hepes (pH 7.5)/0.15 M NaCl/0.01% BSA for selected time intervals between 30 s and 4 min. Residual amidolytic activity was determined by adding 10 $\mu$L of 5 mM S-2288 and monitoring $\Delta A_{405}$/min using the microplate reader. The second-order association rate constant ($k_{assoc}$) was calculated essentially as described (*38*) using the equation

$$\frac{1}{[E]} = k_{assoc}t + \frac{1}{[E_o]} \quad (2)$$

where [E] and [$E_o$] represent the free and total enzyme concentrations, respectively. [E] was calculated by multiplying the percent residual activity by [$E_o$]. The apparent equilibrium inhibition constant ($K_i$) was estimated from the data obtained during titration of PI8 with thrombin as described above by nonlinear regression using UltraFit 3.0 according to the equation for a tight-binding inhibitor, under experimental conditions in which the enzyme in complex with the inhibitor does not contribute to the observed reaction velocity due to the slow dissociation of the complex (*39*):

$$v = \frac{v_o[\sqrt{(K_i + [I] + [E_o])^2 - 4[I][E_o]} - (K_i + [I] - [E_o])]}{2[E_o]} \quad (3)$$

where $v_o$ represents the rate of substrate hydrolysis by the uninhibited enzyme.

*Slow-Binding Inhibition Kinetics.* Inhibition progress curves were obtained under pseudo-first-order conditions by incubating the reactants in 0.5 mL of the buffer used to determine the catalytic constants at 25 °C. Polystyrene cuvettes were previously blocked with 20 mM Hepes (pH 7.5)/0.15 M NaCl/0.1% BSA, and reactions were started by adding the enzyme (0.1 mL) to a solution (0.4 mL) containing the chromogenic substrate and appropriate inhibitor concentration. Reactions for each experiment were started within 30 s, the cuvettes were placed in a Beckman DU-65 spectrophotometer equipped with a six-cell cuvette holder, and multiple reactions were monitored simultaneously at 405 nm. For experiments with factor Xa, the final concentration of the reactants were 0.1 nM factor Xa, 0.8 mM S-2765, and 8, 16, 24, 32, and 40 nM PI8. For experiments with subtilisin A, the final concentration of the reactants were 0.175 nM subtilisin A, 0.8 mM Suc-AAPF-*p*NA, and 1.75, 3.50, 5.25, 7.00, and 8.75 nM PI8. Spontaneous substrate hydrolysis was measured in separate experiments and determined to be negligible. The reactions were allowed to proceed until steady-state velocity was attained, and the data were fitted to the integrated rate equation for slow-binding inhibition (*40*)

$$A = v_s t + (v_o - v_s)\frac{1 - e^{-k't}}{k'} + A_o \quad (4)$$

by nonlinear regression using UltraFit software to obtain values for the initial velocity ($v_o$), the steady-state velocity ($v_s$), the initial absorbance ($A_o$), and the apparent first order rate constant ($k'$) for the establishment of steady-state equilibrium of the proteinase-inhibitor complex. The data obtained from nonlinear regression analysis were then used in various graphical transformations (*39*−*44*) to obtain the inhibition and rate constants for the interactions of PI8 with factor Xa and subtilisin A.

## RESULTS

*Expression and Purification of Recombinant PI8.* The methylotropic yeast *P. pastoris* has been used by several investigators to obtain high expression levels of recombinant proteins. *P. pastoris* is able to metabolize methanol as its sole carbon source through the activity of the enzyme alcohol oxidase. There are two genes that code for alcohol oxidase, *AOX1* and *AOX2*. The *AOX1* gene is responsible for most of the alcohol oxidase activity in the cell, and its expression is tightly regulated by the promoter $P_{AOX1}$. The use of methanol as the sole carbon source in growth medium can induce the expression of alcohol oxidase to levels of ≥30% of the total intracellular soluble protein. Therefore, it is possible to express recombinant proteins at very high levels by replacing the *AOX1* gene with the gene of interest under control of the promoter $P_{AOX1}$ (*45*, *46*).

The PI8 cDNA was subcloned into the *P. pastoris* expression vector pPIC3 to place the cDNA under the control of the promoter $P_{AOX1}$, digested with *Bgl*II to linearize the plasmid DNA and separate the expression cassette from the rest of the vector, and used to transform spheroplasts of the *P. pastoris* strain GS115. More than 50 $His^+$ transformants were obtained and screened for growth characteristics on medium containing methanol as the sole carbon source. Lysates of 32 different $His^+$ transformants were screened for methanol-induced PI8 expression by SDS-PAGE, where PI8 migrated with a molecular mass of ∼45 kDa (data not shown). A single $Mut^s$ transformant was identified that produced high levels of intracellular PI8, approximately 15% of total intracellular soluble protein, as compared with cells that were transformed with the parent pPIC3 vector. The presence of PI8 was confirmed by immunoblotting using rabbit anti-human PI6 IgG as described previously (data not shown) (*25*). A single colony of this transformant was used to inoculate a culture that was scaled up to 2 L to generate biomass before methanol induction. Cells were induced to express PI8 in methanol-containing medium for 5 days at 30 °C. Cells were then harvested, resuspended in a buffer containing high concentrations of protease inhibitors, and broken by using a Bead Beater with zirconia/silica beads.

PI8 was purified to homogeneity from the lysate in a three-step procedure using heparin-agarose column chromatography, Mono Q FPLC, and Mono S FPLC. PI8 was identified in column effluents by a combination of SDS-PAGE, trypsin inhibitory activity, and immunoblotting using rabbit anti-human PI6 IgG as described previously (data not shown) (*25*). PI8 obtained after Mono S FPLC migrated as a single band in SDS-PAGE with an apparent molecular mass of 45 kDa (Figure 1). The purified, putative PI8 was tested for its ability to inhibit the amidolytic activities of trypsin, thrombin, factor Xa, subtilisin A, and *S. aureus* endoproteinase Glu-C. PI8 inhibited the amidolytic activities of trypsin, thrombin, factor Xa, and subtilisin A but failed to inhibit the amidolytic activity of *S. aureus* endoproteinase Glu-C at a 100:1 inhibitor:enzyme molar ratio using Z-FLE-*p*NA as a substrate. Amino-terminal amino acid sequence analysis of the purified PI8 indicated that it, like PI6 (*22*) and PI9 (*25*), was derivitized at the N-terminus. Further treatment of the protein with methanolic HCl revealed that the protein was acetylated at the N-terminus. Inasmuch as PI8 did not demonstrate any inhibitory activity toward the *S. aureus* endoproteinase Glu-C, the purified protein was digested with endoproteinase Glu-C as described (*47*), and the digest fractionated on a $C_4$ reverse phase HPLC column. One HPLC-purified peptide was covalently attached to a Sequelon-AA membrane (Millipore; Bedford, MA) through carboxyl groups and yielded an amino-terminal sequence of AGTV−PLTKL, which is identical to the sequence of residues 150−159 of PI8 as previously deduced (*25*), confirming the identity of the isolated protein as PI8. The

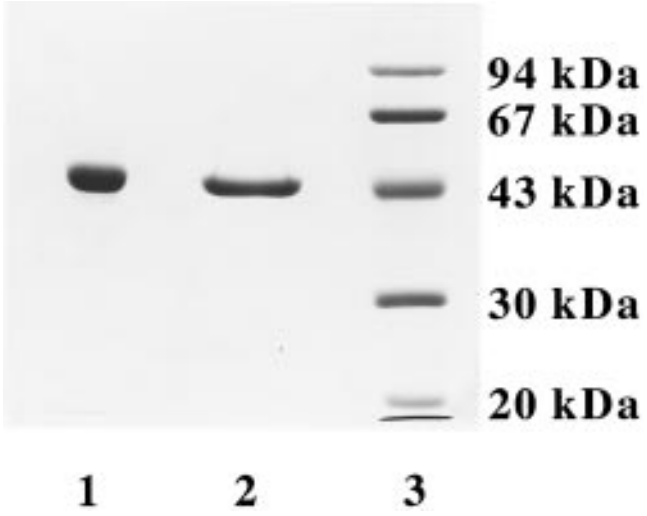


FIGURE 1: Analysis of the purity of PI8. PI8 was subjected to 11% SDS-PAGE and stained with 0.2% Coomassie Blue G-250 in 50% methanol/10% glacial acetic acid after Mono S FPLC: lane 1, PI8 (10 $\mu$g) without the addition of 2-mercaptoethanol; lane 2, PI8 (10 $\mu$g) in the presence of 10% 2-mercaptoethanol; lane 3, mixture of reduced standard proteins including phosphorylase b (94 kDa), bovine serum albumin (67 kDa), ovalbumin (43 kDa), carbonic anhydrase (30 kDa), and soybean trypsin inhibitor (20 kDa).

amino acid in cycle 5 could not be positively identified because of the covalent attachment of the peptide to the membrane through a putative Asp residue at this location.

*Inhibition of Trypsin by PI8*. The presence of heparin had no effect on the inhibitory activity of PI8 with any of the proteinases used in this study. The data obtained describing the rate of product formation were used in various graphical transformations (*48*). On the basis of the results of these transformations, it was determined that PI8 inhibited the amidolytic activity of trypsin by functioning solely as a competitive inhibitor that does not form a tight complex with trypsin. This determination was supported by the observations that the inhibition of trypsin by PI8 did not follow slow-binding kinetics and that incubation of PI8 with trypsin failed to produce a detectable complex by SDS-PAGE. In addition, PI8 appeared to be cleaved by trypsin, as revealed by SDS-PAGE (data not shown). On average, four PI8 molecules were required to form a stable inhibitory complex with one molecule of trypsin, as determined by titration. The data obtained were then used to produce double-reciprocal plots (*36*), where the slope of an individual double-reciprocal plot is equal to $(K_m/v)(1 + [I]/K_i)$. The $K_i$ for the competitive inhibition of trypsin by PI8 was determined to be less than 3.8($\pm$0.2) nM ($n = 4$).

*Inhibition of Thrombin by PI8*. On average, 5000 PI8 molecules were required to form a stable inhibitory complex with one molecule of thrombin, as determined by titration. Data obtained from the analysis of the rate of product formation after various incubation times of thrombin and PI8 were used to create a graphical representation of eq 2 (Figure 2), from which $k_{assoc}$ was calculated directly from the slope of the line. The second-order association rate constant for the complex of PI8 and thrombin was calculated to be 1.0 ($\pm$0.1) $\times$ $10^5$ $M^{-1}$ $s^{-1}$ ($n = 8$). The equilibrium inhibition constant $K_i$ was determined by fitting the data collected from the titration of reactive PI8 with thrombin to eq 3 by nonlinear regression analysis. The $K_i$ for the inhibition of thrombin by PI8 was determined to be 350($\pm$120) pM ($n =$

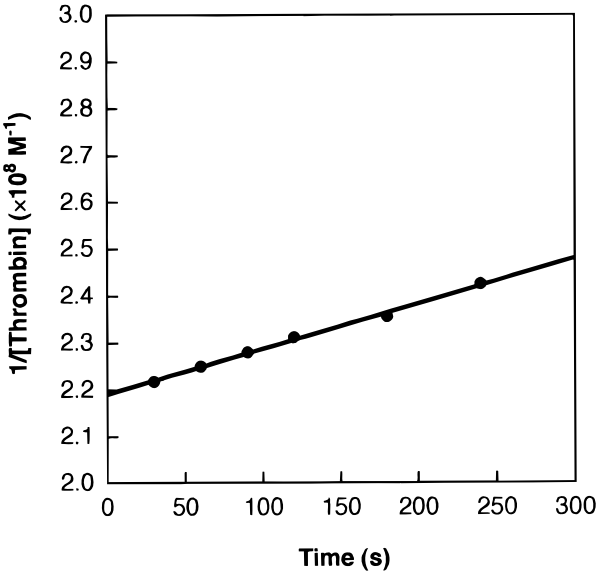


FIGURE 2: Inhibition of human thrombin by PI8 under second-order conditions. Equimolar concentrations (5 nM) of PI8 and human thrombin were incubated for various times at 25 °C and residual thrombin amidolytic activity determined by adding S-2288 and measuring the rate of hydrolysis as a percentage of the rate of an uninhibited control. The association rate constant, $k_{assoc}$, was determined directly from the slope of the line, which was calculated to be 1.0 $\times$ $10^5$ $M^{-1}$ $s^{-1}$.

8). The overall dissociation constant, $k_{dis}$, for the inhibition of thrombin by PI8 was determined according to the relationship $K_i = k_{dis}/k_{assoc}$ to be approximately 3.5 $\times$ $10^{-2}$ $s^{-1}$.

*Inhibition of Factor Xa by PI8*. Preliminary studies indicated that the interaction between PI8 and factor Xa obeyed slow-binding inhibition kinetics, as indicated by the attainment of steady-state equilibrium of the amidolytic activity of factor Xa inhibited by PI8 and the ability to fit the data to eq 4. There are three mechanisms that can describe the slow onset of inhibition (*39*):

$$\mathrm{P} \underset{k_{-1}}{\overset{k_1[\mathrm{I}]}{\rightleftharpoons}} \mathrm{PI} \qquad \text{(A)}$$

$$\mathrm{P} \underset{k_{-1}}{\overset{k_1[\mathrm{I}]}{\rightleftharpoons}} \mathrm{PI} \underset{k_{-2}}{\overset{k_2(\mathrm{slow})}{\rightleftharpoons}} \mathrm{PI}' \qquad \text{(B)}$$

$$\mathrm{P} \underset{k_{-1}}{\overset{k_1(\mathrm{slow})}{\rightleftharpoons}} \mathrm{P}' \underset{k_{-2}}{\overset{k_2[\mathrm{I}]}{\rightleftharpoons}} \mathrm{PI}' \qquad \text{(C)}$$

In mechanism A, the proteinase (P) binds to the inhibitor (I) in a single slow step to form an PI complex. In mechanism B, a loose PI complex is rapidly formed, followed by the slow isomerization to the tight PI′ complex. In mechanism C, the proteinase is assumed to exist in two forms, and active form P and an inactive form P′, which the inhibitor is accessible to. The isomerization of P to P′ is followed by the rapid formation of a tight PI′ complex. These different mechanisms can be distinguished by graphical transformations of the values obtained from the slow-binding kinetic approach (*23, 40*).

On average, 4.5 PI8 molecules were required to form a stable inhibitory complex with one molecule of factor Xa, as determined by titration. The kinetic characterization of PI8 with factor Xa was performed with PI8 concentrations ranging from 80 to 400 times the molar concentration of

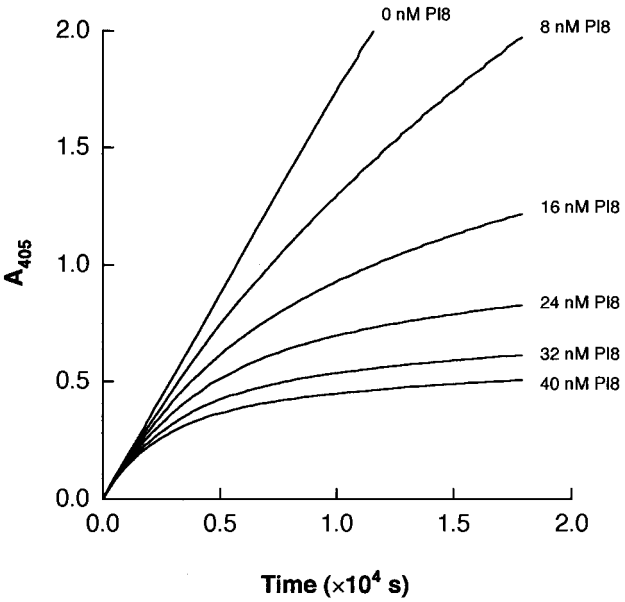


FIGURE 3: Progress curves from slow-binding kinetics for the inhibition of factor Xa by PI8. Factor Xa (0.1 nM) was reacted with 0, 8, 16, 24, 32, and 40 nM PI8 at 25 °C in the presence of 0.8 mM S-2765. The reactions were monitored continuously for 5 h, and the data were fitted to eq 4 to generate values for the variables $\nu_o$, $\nu_s$, $A_o$, and $k'$. To negate any effects of substrate depletion, the upper limit of product formation used to determine the steady-state rates was within the linear range of the uninhibited factor Xa control.

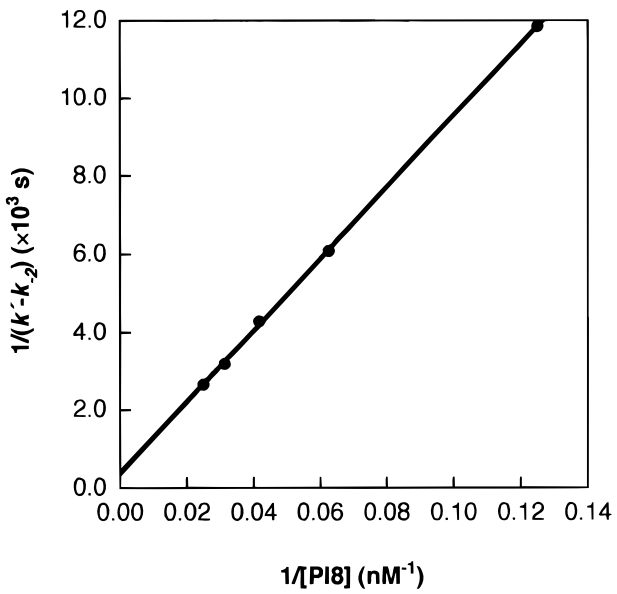


FIGURE 4: $1/(k' - k_{-2})$ versus 1/[PI8] for the interaction of PI8 with factor Xa. Values for $k'$ were generated as described in the legend to Figure 3. The value of $k_{-2}$ was determined by fitting the data obtained from nonlinear regression to eq 4. The line crosses the positive *y*-axis at a point approximately equal to $1/k_2$, indicative of a two-step binding mechanism according to mechanism B (*44*).

factor Xa. A family of inhibition progress curves representative of the reaction between factor Xa and PI8 at the chosen PI8 concentrations is shown in Figure 3. As the concentration of PI8 increased, the initial burst phase of the progress curve shortened and steady-state equilibrium was achieved more readily. Data obtained from the progress curves were fitted to eq 4 by nonlinear regression analysis using UltraFit 3.0 software to obtain values for the variables $\nu_o$, $\nu_s$, $A_o$, and $k'$. The results indicated that the initial velocity, $\nu_o$, was inversely proportional to the concentration of PI8 for each set of progress curves, suggesting that the inhibition of factor Xa by PI8 follows a two-step mechanism described by mechanism B (*40*). This observation was confirmed by plotting $\nu_{max}/\nu_o$ against the PI8 concentration, which exhibited a positive slope (data not shown). The $K_i$ for this interaction can be calculated from the slope of this line using the relationship $\nu_{max}/\nu_o = K_m[I]/[S]K_i + 1 + K_m/[S]$, and was estimated to be 172(±64) nM ($n = 5$). The apparent first-order rate constant $k'$ was found to increase as PI8 concentration increases, which is consistent with only mechanisms A and B. On the basis of these observations, the kinetic constants for the inhibition of factor Xa by PI8 were determined by treating the data according to mechanism B.

The overall second-order association rate constant $k_{assoc}$ was determined by plotting $\log([P]_\infty - [P]_t)$ versus time, where $[P]_\infty = \nu_o/k'$ and $[P]_t$ is the absorbance measured at various times between 0 and 20 min for individual progress curves (data not shown) (*43*). The slope of the lines obtained is equal to $-0.43[I]\{ k_{assoc}/(1 + [S]/K_m )\}$, from which $k_{assoc}$ was calculated to be 7.5(±0.7) × $10^4$ $M^{-1}$ $s^{-1}$ ($n = 5$).

The overall inhibition constant $K_i'$ was determined from plots of both $\nu_{max}/\nu_o$ and $(\nu_o - \nu_s)/\nu_s$ versus PI8 concentration (data not shown). The slopes of these plots are equal to $K_m/[S]K_i'$. $K_i'$ was calculated to be 272(±13) pM ($n = 5$).

To determine the rate constant for the reverse isomerization step ($k_{-2}$) of the factor Xa-PI8 tight complex, a plot of $\nu_{max}/\nu_s$ against PI8 concentration was produced, which was linear (data not shown). $k_{-2}$ was calculated directly from the slope of the line to be 1.4(±0.1) × $10^{-5}$ $s^{-1}$ ($n = 5$). Using the relationship $T_{1/2} = 0.693/k_{-2}$, a half-life of 13.75 h was estimated for the reverse isomerization of the tight complex to the loose complex. The value of the rate constant for the formation of the tight complex $k_2$ was determined by fitting a plot of $k'$ versus PI8 concentration (data not shown) to the equation (*40*)

$$k' = k_{-2} + k_2 \frac{\dfrac{[I]}{K_i}}{1 + \dfrac{[S]}{K_m} + \dfrac{[I]}{K_i}} \qquad (5)$$

by nonlinear regression analysis. By using this method, $k_2$ was estimated to be 11.2(±0.6) × $10^{-3}$ $s^{-1}$ ($n = 5$). In order to verify that the interaction of PI8 and factor Xa occurs by mechanism B and to justify the use of a hyperbola to describe the relationship between $k'$ and [PI8], a double-reciprocal plot of $1/(k' - k_{-2})$ versus 1/[PI8] was generated, using the values obtained from eqs 4 and 5, which is linear for both mechanism A and mechanism B (Figure 4) (*44*). Mechanisms A and B can be differentiated by this approach since in mechanism A the line passes through the origin, whereas in mechanism B the line crosses the positive *y*-axis at a point approximately equal to $1/k_2$. The *y*-intercept of the plot in Figure 4 was used to determine a value of $k_2$ of 2.9(±0.9) × $10^{-3}$ $s^{-1}$ ($n = 5$), which is reasonably close to the value of $k_2$ determined by eq 5. More importantly, the plot in Figure 4 justifies the manipulation of data and determination of kinetic constants according to mechanism B.

*Inhibition of Subtilisin A by PI8.* On average, 50 PI8 molecules were required to form a stable inhibitory complex with one molecule of subtilisin A, as determined by titration. The kinetic characterization of PI8 with subtilisin A was performed with PI8 concentrations ranging from 10 to 50

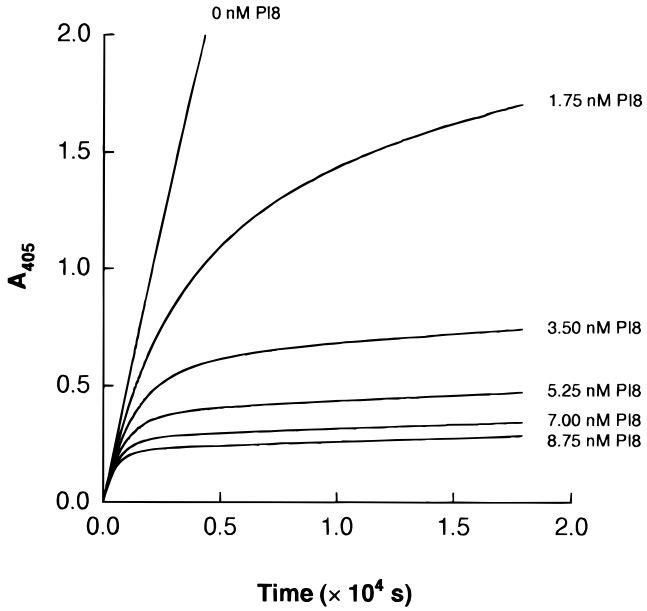


FIGURE 5: Progress curves from slow-binding kinetics for the inhibition of subtilisin A by PI8. Subtilisin A (0.175 nM) was reacted with 0, 1.75, 3.5, 5.25, 7.0, and 8.75 nM PI8 at 25 °C in the presence of 0.8 mM Suc-AAPF-*p*NA. The reactions were monitored continuously for 5 h, and the data were fitted to eq 4 to generate values for the variables $\nu_o$, $\nu_s$, $A_o$, and $k'$. To negate any effects of substrate depletion, the upper limit of product formation used to determine the steady-state rates was within the linear range of the uninhibited subtilisin A control.

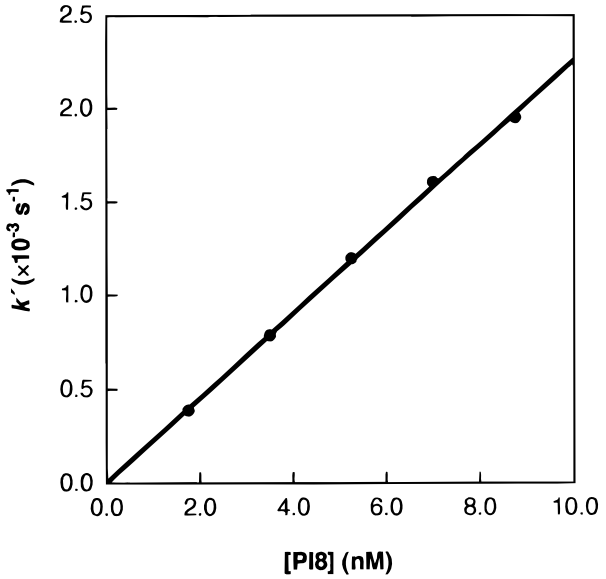


FIGURE 6: Dependence of $k'$ on PI8 concentration for the interaction of PI8 with subtilisin A. The data obtained from nonlinear regression were fitted to eq 6, as described for an interaction according to mechanism A. The second-order association rate constant, $k_1$, for the complex of PI8 and subtilisin A was calculated from the slope of the line.

times the molar concentration of subtilisin A. A family of inhibition progress curves representative of the reaction between subtilisin A and PI8 at the selected PI8 concentrations is shown in Figure 5, and data obtained from the progress curves were fitted to eq 4 by nonlinear regression analysis. The results indicated that the initial velocity, $\nu_o$, was not related to the concentration of PI8 for each set of progress curves, suggesting that the inhibition of subtilisin A by PI8 follows a single-step mechanism described by mechanism A (*40*). This observation was confirmed by plotting $\nu_{max}/\nu_o$ against the PI8 concentration, which had a slope of zero, eliminating mechanism B (data not shown). Furthermore, a plot of $k'$ versus PI8 concentration demonstrated that $k'$ is proportional to PI8 concentration, eliminating mechanism C (Figure 6). Therefore, the data were treated in various ways to determine the kinetic constants for the inhibition of subtilisin A by PI8 according to mechanism A.

The apparent second-order association rate constant $k_1$ for the complex of PI8 and subtilisin A was calculated by fitting the data obtained from nonlinear regression analysis to the equation (*40*)

$$k' = k_{-1} + \frac{k_1[\mathrm{I}]}{1 + \dfrac{[\mathrm{S}]}{K_m}} \qquad (6)$$

which predicts a linear relationship between $k'$ and [PI8]. From the slope of the line (Figure 6), $k_1$ was calculated to be 1.16(±0.03) × $10^6$ $M^{-1}$ $s^{-1}$ ($n$ = 5). Due to the degree of error present and its apparent small value, $k_{-1}$ was not determined from the *y*-intercept of the line, but rather directly from the slope of the line generated using the relationship $k' = k_{-1}(\nu_o/\nu_s)$ (data not shown) (*40*). The value of $k_{-1}$ was calculated to be 1.06(±0.23) × $10^{-5}$ $s^{-1}$ ($n$ = 5). This translates to a half-life of 18.16 h for the PI8−subtilisin A complex.

The equilibrium inhibition constant $K_i$ was determined by plotting values of $\nu_{max}$ and $\nu_s$ obtained from nonlinear regression analysis against PI8 concentration according to the relationships $\nu_{max}/\nu_s = 1 + [\mathrm{I}]/K_{iapp}$ and $K_i = K_{iapp}/(1 + [\mathrm{S}]/K_m)$. From the slope of the line generated (data not shown), $K_i$ was calculated to be 8.6(±0.4) pM ($n$ = 5). In order to verify that the interaction of PI8 and subtilisin A occurs by mechanism A and to justify the use of a line to describe the relationship between $k'$ and [PI8], a double-reciprocal plot of $1/(k' - k_{-1})$ versus 1/[PI8] was created (Figure 7). The line did not cross the positive *y*-axis and passed through the origin, as expected for inhibition according to mechanism A.

## DISCUSSION

In the present study, we have successfully expressed, purified, and determined the inhibitory properties of the novel human intracellular proteinase inhibitor designated as PI8. PI8 inhibited the amidolytic activity of porcine trypsin with a $K_i$ of less than 3.8 nM but was unable to form a tight complex with this proteinase. The depletion of inhibitor seen during titration of PI8 with trypsin supports this observation, since PI8 is most likely cleaved at various sites, including those within the reactive site loop, and efficiently released during its interaction with trypsin. Interestingly, the mechanism of PI8 inhibition of trypsin differs greatly from that of the inactivation of trypsin by PI6 (*23*), a serpin that shares 63% sequence identity with PI8, including an identical arginine residue in the $P_1$ position in the reactive site loop (*25*). This suggests that sequence divergence in the reactive site loop between PI8 and PI6 is responsible for the unique mechanisms for the inactivation of trypsin. There are also inherent difficulties in the determination of the $K_i$ for the interaction of PI8 and trypsin, since PI8 is not a tight-binding inhibitor of trypsin. It is also possible that there are some

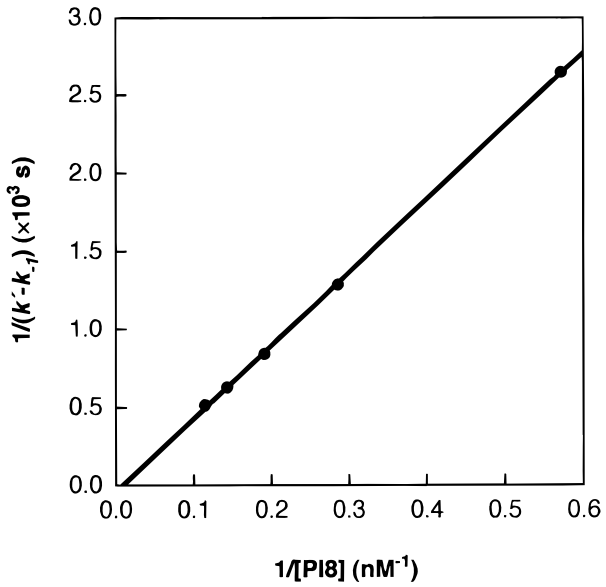


FIGURE 7: $1/(k' - k_{-1})$ versus 1/[PI8] for the interaction of PI8 with subtilisin A. Values for $k'$ were generated as described in the legend to Figure 5. Values for $k_{-1}$ were calculated from the slope of the line generated according to the relationship $k' = k_{-1}(\nu_o/\nu_s)$ (*40*). The line does not cross the positive *y*-axis and passes through the origin, indicative of a single-step binding mechanism according to mechanism A (*44*).

species of PI8 cleaved and released by trypsin that are still able to function as competitive inhibitors of trypsin, if cleavage is occurring at sites other than those within the reactive site loop. For these reasons, the equilibrium inhibition constant for the unique inhibition of trypsin by PI8 is expressed only as an upper limit. Conversely, PI8 was able to form a tight inhibitory complex with a $K_i$ of 350 pM with human thrombin and an overall $K_i'$ of 272 and 8.6 pM with human factor Xa and subtilisin A, respectively. In addition, the respective second-order association rate constants for the formation of the complexes with thrombin, factor Xa, and subtilisin A were $1.0 \times 10^5$, $0.75 \times 10^5$, and $1.16 \times 10^6$ $M^{-1}$ $s^{-1}$, demonstrating that PI8 is a potent inhibitor of these proteinases, especially subtilisin A.

PI8 was tested for its ability to form SDS-stable complexes with the proteinases listed in this study. PI8 was able to form an SDS-stable complex with human thrombin and human factor Xa, but was unable to form an SDS-stable complex with subtilisin A, a proteinase that PI8 rapidly and efficiently inactivates. In addition, PI8 appeared to be cleaved following incubation with trypsin. The enzyme-inhibitor complex, as seen by SDS-PAGE, reflects a complex stabilized by an acyl−ester linkage between the active-site serine of the proteinase and the carbonyl of the $P_1$ residue of the cleaved serpin. However, evidence exists that acyl−ester linkage seen after treatment with SDS is most likely an artifact (*2*, *49*, *50*). The inhibitory structure of serpins is conformationally unstable, and the reactive site loop is highly susceptible to cleavage by proteinases that they do or do not inhibit. During the titration of PI8 with the selected enzymes used in this study, it was observed that the PI8 preparations were not completely active on a mass basis. This phenomenon was not due to proteolytic inactivation of PI8, but most likely the disproportionate pathway that dictates the binding of serpins to some proteinases, since the exposed nature of the reactive site loop enables the serpin to act as either a substrate or an inhibitor for a proteinase, or both. This phenomenon has been observed for the interactions of $\alpha_1$-antichymotrypsin and $\alpha_1$-proteinase inhibitor with human mast cell chymase (*51*), C1 inhibitor with plasma kallikrein (*52*), and $\alpha_2$-antiplasmin with trypsin and chymotrypsin (*53*) and is a recognized characteristic of some of the interactions that occur between proteinases and serpins. This suggests that several serpin molecules are required to inhibit a single proteinase molecule in order to overcome the inactivation of many of the serpin molecules during the reaction. As long as the inhibitor is in excess of the enzyme, efficient inhibition can occur. This phenomenon may be relevant as to why high levels of cytoplasmic PI9 antigen are observed in placental tissue by immunohistochemical methods,[2] consistent with the high levels of PI9 mRNA observed by Northern blot analysis (*25*).

PI8 shares a high degree of sequence identity and structural features unique to members of the ovalbumin family of serpins, most notably the absence of a cleavable N-terminal signal sequence (*25*). However, several structures within the primary structure of ovalbumin have been demonstrated to function as an internal signal sequence (*54*−*56*). Previous studies have also demonstrated that PAI-2 can be glycosylated and exported by monocytes upon activation by phorbol esters (*15*) and that SCCA is secreted in a glycosylated form by carcinoma squamous epithelial cells, while SCCA in normal squamous epithelial cells remains cytoplasmic (*16*). This information coupled with the findings that PI8 has consensus sites for the potential attachment of an N-linked carbohydrate cannot eliminate the possibility that the functions of PI8, as well as those of the other ovalbumin-type serpins, are not strictly confined to the cytoplasm.

The strong interaction between PI8 and subtilisin A was most intriguing, since subtilisin A is evolutionarily divergent from the trypsin-like serine proteinases (*57*) and the prototype for several mammalian dibasic endoproteinases. The first and most highly characterized of these mammalian subtilisin-like endoproteinase is furin, a ubiquitous, membrane-bound calcium-dependent serine proteinase involved in the processing of precursor proteins within the exocytic and endocytic pathways (*58*−*60*). Furin is also a prominent processor and activator of viral glycoproteins, which has been demonstrated to be a critical factor in determining organ and host tropism, the spread of viral infection, and pathogenicity (*61*, *62*). Previous studies have demonstrated that furin is inhibited by $\alpha_1$-antitrypsin, an engineered variant of EI (*63*), and by antithrombin III in the presence of heparin (*64*). In this regard, the results of preliminary studies indicate that PI8 readily inhibits soluble recombinant furin in a slow-binding manner and also forms an SDS-stable complex with this proteinase.[3] In addition, preliminary immunoblotting and inhibition studies indicate that a measurable amount of PI8 is being secreted into the conditioned medium of BHK cells stably-transfected with PI8 cDNA (*25*).[2] The characterization of PI8 as a potent inhibitor of the prototypical proteinase subtilisin A, as well as its potential secretion and inhibition of the prototypical mammalian endoproteinase furin, suggests that PI8 may be a physiological regulator of one or more subtilisin-type dibasic pro-protein processing endoproteinases.

[2] Dahlen, J. R., & Kisiel, W, unpublished observations.

[3] Dahlen, J. R., Jean, F., Thomas, G., Foster, D. C., & Kisiel, W, manuscript in preparation.

## ACKNOWLEDGMENT

We greatly appreciate the assistance of Dr. Andrzej Pastuszyn (University of New Mexico, Protein Chemistry Laboratory) for performing HPLC and amino acid sequencing.

## REFERENCES

1. Huber, R., & Carroll, R. W. (1989) *Biochemistry 28*, 8951−8966
2. Potempa, J., Korzus, E., & Travis, J. (1994) *J. Biol. Chem. 269*, 15957−15960.
3. Cohen, A. B., Geczy, D., & James, H. L. (1987) *Biochemistry 17*, 392−400.
4. Loderman, H., Tokuoka, R., Deisenhofer, J., & Boswell, D. R. (1984) *J. Mol. Biol. 177*, 531−556.
5. Schechter, I., & Berger, A. (1967) *Biochem. Biophys. Res. Commun. 27*, 157−162.
6. Bode, W., & Huber, R. (1992) *Eur. J. Biochem. 204*, 433−451.
7. Bjork, I., Nordling, K., Larsson, I., & Olson, S. T. (1992) *J. Biol. Chem. 267*, 19047−19050.
8. Bjork, I., Nordling, K., & Olson, S. T. (1993) *Biochemistry 32*, 6501−6505.
9. Skiver, K., Wikoff, W. R., Patston, P. A., Tausk, F., Schapira, M., Kaplan, A. P., & Bock, S. C. (1991) *J. Biol. Chem. 266*, 9216−9221.
10. Flint, I. L., Bailey, T. J., Gustafson, T. A., Maekham, B. E., & Morkin, E. (1986) *Proc. Natl. Acad. Sci. U.S.A. 83*, 7708−7712.
11. Doolittle, R. F. (1983) *Science 222*, 417−419.
12. Hunt, L. T., & Dayhoff, M. O. (1980) *Biochem. Biophys. Res. Commun. 95*, 864−871.
13. Scott, F. L., Coughlin, P. B., Bird, C., Cerruti, L., Hayman, J. A., & Bird, P. (1996) *J. Biol. Chem. 271*, 1605−1612.
14. Sun, J., Bird, C., Sutton, V., McDonald, L., Coughlin, P. B., De Jong, T. A., Trapani, J. A., & Bird, P. (1996) *J. Biol. Chem. 271*, 27802−27809.
15. Belin, D., Wohlwend, A., Schleuning, W. D., Kruithof, E. K. O., & Vassali, J.D. (1989) *EMBO J. 8*, 3287−3294.
16. Suminami, Y., Kishi, F., Sekiguchi, K., & Kato, H. (1991) *Biochem. Biophys. Res. Commun. 181*, 51−58.
17. Sheng, S., Carey, J., Seftor, E. A., Dias, L., Hendrix, M. J. C., & Sager, R. (1996) *Proc. Natl. Acad. Sci. U.S.A. 93*, 11669−11674.
18. Ye, R. D., Ahern, S. M., Le Beau, M. M., Lebo, R. V., & Sadler, J. E. (1989) *J. Biol. Chem. 264*, 5495−5502.
19. Dubin, A., Travis, J., Enghild, J. J., & Potempa, J. (1992) *J. Biol. Chem. 267*, 6576−6583.
20. Remold-O'Donnell, E., Chin, J., & Alberts, M. (1992) *Proc. Natl. Acad. Sci. U.S.A. 89*, 5635−5639.
21. Zou, Z., Anisowicz, A., Hendrix, M. J. C., Thor, A., Neveu, M., Sheng, S., Rafidi, K., Seftor, E., & Sager, R. (1994) *Science 263*, 526−529.
22. Morgenstern, K. A., Henzel, W. J., Baker, J. B., Wong, S., Pastuszyn, A., & Kisiel, W. (1993) *J. Biol. Chem. 268*, 21560−21568.
23. Morgenstern, K. A., Sprecher, C., Holth, L., Foster, D., Grant, F. J., Ching, A., & Kisiel, W. (1994) *Biochemistry 33*, 3432−3441.
24. Coughlin, P. B., Tetaz, T., & Salem, H. H. (1993) *J. Biol. Chem. 268*, 9541−9547.
25. Sprecher, C. A., Morgenstern, K. A., Mathewes, S., Dahlen, J. R., Schrader, S. K., Foster, D. C., & Kisiel, W. (1995) *J. Biol. Chem. 270*, 29854−29861.
26. Schick, C., Kamachi, Y., Bartuski, A. J., Cataltepe, S., Schechter, N. M., Pemberton, P. A., & Silverman, G. A. (1997) *J. Biol. Chem. 273*, 1849−1855.
27. Riewald, M., & Schleef, R. R. (1995) *J. Biol. Chem. 270*, 26754−26757.
28. Takeda, A., Yamamoto, T., Nakamura, Y., Takahashi, T., & Hibino, T. (1995) *FEBS Lett. 359*, 78−80.
29. Faller, B., Cadene, M., & Bieth, J. G. (1993) *Biochemistry 32*, 9230−9235.
30. Kisiel, W., & Davie, E. W. (1975) *Biochemistry 14*, 4928−4934.
31. Kisiel, W., Smith, K. J., & McMullen, B. A. (1985) *Blood 66*, 1302−1308.
32. Kondo, S., & Kisiel, W. (1987) *Blood 70*, 1947−1954.
33. Mahoney, W. C., Kurachi, K., & Hermodson, M. A. (1980) *Eur. J. Biochem. 105*, 545−552.
34. Laemmli, U. K. (1970) *Nature 227*, 680−685.
35. Chase, T., & Shaw, E. (1967) *Biochem. Biophys. Res. Commun. 29*, 508−514.
36. Chase, T., & Shaw, E. (1967) *Biochemistry 8*, 2212−2224.
37. Hill, A. V. (1910) *J. Physiol. Lond. 40*, iv.
38. Beatty, K., Bieth, J., & Travis, J. (1980) *J. Biol. Chem. 255*, 3931−3934.
39. Cha, S. (1975) *Biochem. Pharmacol. 24*, 2177−2185.
40. Morrison, J. F., & Walsh, C. T. (1988) *Adv. Enzymol. 61*, 201−301.
41. Longstaff, C., & Gaffney, P. J. (1991) *Biochemistry 30*, 979−986.
42. Morrison, J. F. (1982) *Trends Biochem. Sci. 7*, 102−105.
43. Tian, W.-X., & Tsou, C.-L. (1982) *Biochemistry 21*, 1028−1032.
44. Shapiro, R., & Riordan, J. F. (1984) *Biochemistry 23*, 5234−5240.
45. Cregg, J. M., Vedvick, T. S., & Raschke, W. C. (1993) *Bio/Technology 11*, 905−910.
46. Sreekrishna, K., Potenz, R. H. B., Cruze, J. A., McCombie, W. R., Parker, K. A., Nelles, L., Mazzaferro, P. K., Holden, K. A., Harrison, R. G., Wood, P. J., Phelps, D. A., Hubbard, C. E., & Fuke, M. (1988) *J. Basic Microbiol. 28*, 265−278.
47. Houmard, J., & Drapeau, G. R. (1972) *Proc. Natl. Acad. Sci. U.S.A. 12*, 3506−3509.
48. Tipton, K. F. (1996) in *Enzymology Labfax* (Engel, P. C., Ed.) pp 115−174.
49. Shieh, B. H., Potempa, J., & Travis, J. (1989) *J. Biol. Chem. 264*, 13420−13423.
50. Matheson, N. R., van Halbeek, H., & Travis, J. (1991) *J. Biol. Chem. 266*, 13489−13491.
51. Schechter, N. M., Sprows, J. L., Schoenberger, O. L., Lazarus, G. S., Cooperman, B. S., & Rubin, H. (1989) *J. Biol. Chem. 264*, 21308−21315.
52. Patston, P. A., Gettins, P., Beechem, J., & Schapira, M. (1991) *Biochemistry 30*, 8876−8882.
53. Enghild, J. J., Valnickova, Z., Thogersen, I., Pizzo, S., & Salvesen, G. (1993) *Biochem. J. 291*, 933−938.
54. Lingappa, V. R., Lingappa, J. R., & Blobel, G. (1979) *Nature 281*, 117−121.
55. Meek, R. L., Walsh, K. A., & Palmiter, R. D. (1982) *J. Biol. Chem. 257*, 12245−12251.
56. Tabe, L., Krieg, P., Strachan, R., Jackson, D., Wallis, E., & Colman, A. (1984) *J. Mol. Biol. 180*, 645−666.
57. Neurath, H. (1984) *Science 224*, 350−357.
58. Barr, P. J., Mason, O. B., Landsberg, K. E., Wong, P. A., Kiefer, M. C., & Brake, A. J. (1991) *DNA Cell Biol. 10*, 319−328.
59. Wise, R. J., Barr, P. J., Wong, P. A., Kiefer, M. C., Brake, A. J., & Kaufman, R. J. (1990) *Proc. Natl. Acad. Sci. U.S.A. 87*, 9378−9382.
60. Denault, J.-B., & Leduc, R. (1996) *FEBS Lett. 379*, 113−116.
61. Klenk, H.-D., & Rott, R. (1988) *Adv. Virus Res. 34*, 247−281.
62. Garten, W., Hallenberger, S., Ortmann, D., Schafer, W., Vey, M., Angliker, H., Shaw, E., & Klenk, H. D. (1994) *Biochimie 76*, 217−225.
63. Anderson, E. D., Thomas, L., Hayflick, J. S., & Thomas, G. (1993) *J. Biol. Chem. 268*, 24887−24891.
64. Brennan, S. O., & Nakayama, K. (1994) *FEBS Lett. 338*, 147−151.

BI970977P